

Addendum 4: Presented at the Air and Waste Management Association International Specialty Conference 'Visibility and Fine Particles', October 1989, Estes Park, CO.

APPLICATION OF A DIFFERENTIAL MASS BALANCE MODEL TO ATTRIBUTE SULFATE HAZE IN THE SOUTHWEST

Douglas A. Latimer
Latimer & Associates
679 Quince Circle
Boulder, Colorado 80304

Hari K. Iyer
Department of Statistics
Colorado State University
Fort Collins, Colorado 80523

William C. Malm
National Park Service
CIRA, Foothills Campus
Fort Collins, Colorado 80523

Abstract

As part of the Winter Haze Intensive Experiment (WHITEX), the contribution of a large, coal-fired power plant, the Navajo Generating Station (NGS), to ambient sulfur and regional visibility impairment was studied. One of the main quantitative attribution techniques used was a Differential Mass Balance (DMB) Model. The DMB model is a receptor model combined with elements of a deterministic model designed to calculate the fraction of an ambient species contributed by an emissions source. The DMB model was applied to ambient concentrations of sulfur species (SO_2 and SO_4^{2-}) measured at Hopi Point in Grand Canyon National Park and at Page, Arizona in the Glen Canyon National Recreation Area. Central to the DMB model application is the selection of dry deposition rates (k_1 and k_2) and SO_2 oxidation rates (k_c). First, the literature was surveyed to assess the range of plausible deposition and oxidation rates. Then, an optimization procedure was devised and applied to determine the rates that would best explain the observed data. The optimized rates were entirely consistent with the literature values. NGS, on average, was found to contribute 71 percent of the ambient sulfate measured at Hopi Point during the WHITEX study.

APPLICATION OF A DIFFERENTIAL MASS BALANCE MODEL TO ATTRIBUTE SULFATE HAZE IN THE SOUTHWEST

Introduction

The Differential Mass Balance (DMB) model is a receptor model combined with elements of a deterministic model which is designed to calculate the fraction of an ambient species contributed by an emissions source. The concentration of the given species contributed by the source is calculated by scaling the ambient concentration of tracer by the ratio of the emission rates of the species of interest to the tracer, multiplied by a factor which accounts for deposition and conversion of the species of interest. The name "differential mass balance" refers to the fact that conversion and deposition of a species of interest may differ from that for a tracer; thus, the difference in mass resulting from deposition and conversion during the time from emission to measurement at a receptor site must be determined. In the current application, to the Navajo Generating Station (NGS) in January-February 1987, the species of interest are sulfur dioxide (SO_2) and sulfate (SO_4^-) and the tracer is deuterated methane (CD_4).

Malm et al.^{1,2} describe the equations used in the DMB analysis. The application of DMB requires estimation of deposition and oxidation rates. The first step was to survey the literature to find the range of such rates reported at other locations. Then, an optimization procedure was applied to this range to make best estimates.

Dry Deposition

Dry deposition is the process of mass transfer by which trace gases and particles are removed from the atmosphere to the surfaces of soil, rock, vegetation, and water bodies. Deposition involves a series of processes starting with atmospheric diffusion to the ground surface followed by various physical, chemical, and biological processes. Hicks³ provides an excellent overview of the important processes in dry deposition. Wesely⁴ presents a detailed parameterization of the various elements that control dry deposition rates.

Dry deposition is commonly characterized by the deposition velocity v_d which is defined as the ratio of the flux F of material to the earth's surface and the ambient atmospheric concentration C of the species. Deposition velocities are generally highest during the day when atmospheric mixing is strongest and leaf stomata of vegetation are open.

Tables in the full report of this work¹ present the range of deposition velocities that have been measured for different surfaces for SO_2 and submicron particles such as SO_4^- and references. Deposition velocities for SO_2 range from 0.1 to 2.3 cm/s, with a median value of 0.7 cm/s. Deposition velocities for fine particles range from 0 to 1.0 cm/s, with a median value of 0.2 cm/s.

Sulfur Oxidation

Most ambient SO_4^- is produced from the oxidation in the atmosphere of emitted SO_2 . Thus, the contribution of an SO_2 source to ambient sulfate is dependent both on the SO_2 emission rate and the rate at which SO_2 is oxidized to

sulfate. Although SO_2 oxidation rates in the NGS plume were not directly measured, the TMBR analysis of WHITEX data¹ indicated that data can be best fit by an oxidation rate which varies linearly with relative humidity (i.e., $k_c = C \text{ RH}$, where k_c , in percent per hour, is the pseudo-first-order rate constant for SO_2 oxidation to SO_4^{2-} , C is a constant, and RH is the relative humidity in percent). The TMBR analysis also indicated that oxidation rates, especially during humid conditions, can be greater than 1 percent per hour.¹ The oxidation rates in the range 1-2 percent per hour during WHITEX, determined on the basis of TMBR (and also DMB, see below), are much higher than those reported by Richards et al.⁵ in a previous study of the NGS plume. They had found maximum noontime SO_2 oxidation rates of 0.8 percent per hour in summer and 0.2 percent per hour in winter, with 24-hour average rates much lower than these maxima. However, all of these measurements were made during cloud-free conditions, when gas-phase chemical reactions were the only major oxidation pathway. The measurements of Richards et al.⁵ are consistent with theoretical calculations of SO_2 oxidation rates calculated from equilibrium concentrations of hydroxyl (OH) radical.¹

However, aqueous-phase oxidation can be much faster than gas-phase oxidation.^{6,7} Reactions in water droplets with the following species can cause rapid SO_2 oxidation: ozone (O_3), hydrogen peroxide (H_2O_2), iron (Fe), manganese (Mn), carbon (C), nitrous acid (HNO_2), and nitrogen dioxide (NO_2). All reactions, except the one with H_2O_2 , which remains rapid at all pH's, are quenched as the droplet becomes more acidic (from production of sulfuric acid). Field measurements of SO_2 oxidation in power plant plumes indicate that oxidation rates are often much faster than what can be accounted for with gas-phase processes.⁶ Even higher rates have been observed when a plume passes through a cloud or fog bank.⁷ Aqueous-phase oxidation is a plausible explanation for the relatively high rates of SO_2 oxidation inferred from the TMBR analysis¹ and the DMB analysis (as discussed below). The wintertime period was characterized by frequent presence of clouds, fog, and cooling tower plumes,¹ which would provide water droplets for aqueous-phase oxidation. At Hopi Point in the Grand Canyon, the average humidity during WHITEX was 48 percent, with a maximum of 97 percent.¹ Thus, it is not surprising that the empirical fit (TMBR model¹) of SO_2 oxidation rate is proportional to relative humidity. The amount of water associated with hygroscopic aerosol increases with increasing humidity. Also, clouds, fog, and cooling tower plumes are more likely to occur at higher humidities.

The numerous studies referenced above support the possibility for rapid SO_2 oxidation in power plant plumes, especially during humid conditions. However, the question remains as to whether there is sufficient oxidant in the Southwest during winter to explain the SO_2 oxidation rates inferred from the TMBR analysis. The potential rate of SO_2 oxidation can be appreciated by considering just the reactions with H_2O_2 . A series of measurements were made by Van Valin et al.⁸ during February 1987 along the 91.5 degree meridian from Iowa to the Gulf of Mexico. They found H_2O_2 concentrations varied inversely with latitude, with values in the range from <0.1 to 1.0 ppb. At the latitude of the Grand Canyon (36 degrees), they found H_2O_2 concentrations in the range from 0.1 to 0.6, centered on 0.3 ppb. They also found that H_2O_2 concentrations were dependent upon air mass history; air masses transported from lower latitudes generally had higher peroxide concentrations. Using these measured rates and the data summarized by Seinfeld,⁶ we find that oxidation rates greater than 100 percent per hour are possible for the short period required to use up available H_2O_2 . Since one mole of H_2O_2 is consumed for each mole of SO_2 oxidized, the average

peroxide concentration of 0.3 ppb can produce $0.4 \mu\text{g}/\text{m}^3$ of sulfate as sulfur ($1.2 \mu\text{g}/\text{m}^3$ as sulfate). Of course, higher concentrations of sulfate can be produced when air masses are more H_2O_2 -rich and as additional H_2O_2 is produced. Thus, it appears that rapid SO_2 oxidation suggested by the TMBR analysis¹ can be supported by theoretical aqueous-phase mechanisms and known concentrations of just one of the possible oxidants (H_2O_2).

Evidence for aqueous-phase oxidation is available in the particle size distribution data collected during WHITEX.¹ When particle size distributions were stratified by relative humidity, a larger fraction of the total fine particle mass was in the $0.5 \mu\text{m}$ size range at the higher humidities. At lower humidities a relatively greater fraction of particles were found in the range 0.1 to $0.3 \mu\text{m}$. Hering and Friedlander⁹ found that sulfate in Los Angeles consisted of two sizes: (1) one at $0.2 \mu\text{m}$, was found to be associated with sulfate formed from gas-phase oxidation and (2) one at $0.5 \mu\text{m}$ was found to be due to aqueous-phase oxidation. McMurry and Wilson¹⁰ used aerosol growth data versus particle size to infer the relative importance of gas- and aqueous-phase oxidation mechanisms: growth in the $0.5 \mu\text{m}$ size range resulted mainly from aqueous-phase oxidation. Thus, the particle size data from WHITEX is consistent with the aqueous-phase oxidation mechanism.

Optimization of Deposition and Oxidation Rates

The literature review of deposition and oxidation rates supported quite a wide range of possible rates (i.e., deposition velocities ranging from 0.1 to 2.3 cm/s for SO_2 and 0 to 0.9 for sulfate, and oxidation rates from 0 to >100 percent per hour). The DMB model was optimized by selecting combinations of deposition and oxidation parameters that explained the most variance in the measured sulfate data at Hopi Point. The full range of literature deposition rates was tested. Since the TMBR analysis had suggested that oxidation rates were proportional to relative humidity (RH) and in the range from 1 - 2 percent per hour,¹ sulfur oxidation rates were varied over a smaller range than the literature values: such that $k_c = C * (\text{RH}/100\%)$ where $0 < C < 4$ percent per hour.

The optimization was carried out by exercising the DMB model for all combinations of the following three parameters:

Deposition velocity for SO_2 : $v_1 = 0.1$ to 2.3 cm/s in increments of 0.1 cm/s (23 values).

Deposition velocity for sulfate: $v_2 = 0.0$ to 0.9 cm/s in increments of 0.05 cm/s (19 values).

SO_2 Conversion (at 100% RH): $C = 0.0$ to 4.0% /h in increments of 0.5% /h (9 values).

Thus, a total of 3,933 different combinations of these three fundamental parameters ($23 \times 19 \times 9$) were used in separate DMB calculations for each 12-hour period of data for Hopi Point. The deposition velocities were used in combination with an assumed mixing height (H_m) of 700 meters (the sum of the NGS effective stack height of 600 m plus 100 m of vertical diffusion¹) to determine the deposition rates (k_1 and k_2). The NGS plume age used in these

calculations was derived from a meteorological analysis of plume position as a function of time during WHITEX.¹

The measured total ambient sulfate concentration $C_{SO_4,k}$ for each time period k was regressed against the measured and scaled NGS tracer concentration (C_{CD_4}) and the ambient arsenic concentration ($C_{As,k}$), a tracer for copper smelters, using a linear regression model of the form:

$$C_{SO_4,k} = C_0 + \beta_{CD_4}(RH_k) C_{CD_4,k} + \beta_{As} RH_k C_{As,k} ,$$

where C_0 is the background (non-NGS and non-smelter) SO_4^{2-} concentration, $\beta_{CD_4}(RH_k)$ is the coefficient for the tracer concentration $C_{CD_4,k}$ at time period k , derived from the DMB calculations of oxidation and deposition,^{1,2} and β_{As} is the coefficient for the arsenic tracer for smelters. The contributions of NGS and smelters are assumed to be functions of the relative humidity (RH_k) at time period k .

All combinations of deposition velocities for SO_2 and sulfate and C were identified such that the regression model R^2 was 0.70 or greater. Out of the 3,933 combinations of parameters tested, 676 combinations were found to provide R^2 greater than 0.7. The DMB results using this smaller set of parameter values were assumed to represent the range of plausible NGS contributions.

Figure 1 shows the combinations of deposition velocities with $R^2 > 0.70$ for an assumed oxidation rate of $1.5\%/h \times RH/100$. This figure indicates that many different combinations of deposition velocities yield R^2 values greater than 0.70. However, higher SO_2 deposition velocities are combined with lower sulfate deposition velocities, and vice versa. The highest R^2 (0.82) was achieved with deposition velocities for SO_2 and sulfate of 0.98 and 0.08 cm/s (see the X in Figure 1) and a oxidation rate (C) of 1.7 percent/hour. The empirically optimum deposition rates are consistent with the median of the literature deposition velocities, 0.70 and 0.20 cm/s (see the + in Figure 1).

Application of the DMB Model With Optimized Parameters

This optimum set of deposition and conversion parameters produced an average NGS contribution to sulfate at Hopi Point of 71 percent over the WHITEX experimental period for which tracer data were available. Figure 2 shows the computed average NGS fraction of total sulfate at Hopi Point for all 676 combinations of deposition velocities and oxidation rates producing $R^2 > 0.70$. Although the average NGS fraction of total sulfate is 0.71 for the combination of parameters that gives the highest R^2 (= 0.82), the NGS fraction of total sulfate ranges from 0.38 to 1.14 for all combinations of parameters with $R^2 > 0.70$. Thus, NGS on average is calculated to contribute 71 (+29, -33) percent of the ambient sulfate measured at Hopi Point during the WHITEX period.

Table I shows the history of the total sulfate, the NGS sulfate, and the NGS fraction of total ambient sulfate during the WHITEX period. The table shows uncertainties associated with: (1) the range of deposition velocities and oxidation rates that yield $R^2 > 0.70$; and (2) the measurement uncertainties (including the uncertainty in plume age, which was estimated to be ± 20 percent). Since the two categories of uncertainty are expected to be independent, the total uncertainty (standard error) is calculated from the square root of the sum of the squares:

$$E_{\text{total}} = (E_k^2 + E_m^2)^{1/2}.$$

Figure 3(a) shows the best estimate of the NGS sulfate and fraction as a function of time. Figure 3(b) shows the uncertainty range on these estimates, calculated by taking plus or minus twice the total standard error E_{total} . While the best estimates of the NGS contribution is at times greater than the maximum possible (100 percent), the uncertainty bars span physically possible values of NGS's contribution (i.e., 0-100 percent).

The optimized DMB model was tested on both SO_2 and sulfate concentrations at Hopi Point using different estimates of the NGS plume age.¹ The following three NGS plume ages were tested: the minimum estimated plume age, the larger of 12 hours or the minimum NGS plume age, and the maximum plume age. The NGS sulfate fraction varies from 72 to 87 percent over the range of assumed NGS plume ages. However, only the maximum estimate of NGS plume ages yielded NGS SO_2 contributions that are physically meaningful (i.e., < 100%).

Summary of Conclusions

The DMB model was applied to the ambient sulfur data collected in Grand Canyon National Park during January-February 1987. On average, the DMB model found that the Navajo Generating Station contributed 71 percent of the ambient sulfate in the park during this period. Nearly all of the sulfur species measured in Page was attributed to the plant. The deposition and SO_2 oxidation rates used in the DMB model were optimized, and these values were found to be consistent with literature values. Oxidation rates observed during the study (on the order of 1 percent per hour) can only be explained by aqueous-phase chemical mechanisms; gas-phase oxidation rates in winter are very small. The humidity-dependent oxidation rate observed during WHITEX can be explained by the fact that water droplets (clouds, fog, and cooling tower plumes) would be more ubiquitous during high humidity conditions. Figure 4 illustrates the optimized DMB model calculations of the distribution of emitted sulfur from the NGS as a function of plume parcel age; the distribution is among SO_2 in the air, SO_2 deposited, sulfate airborne, and sulfate deposited. For typical plume ages, approximately 10-15 percent of emitted sulfur is left in the air as sulfate.

References

1. W. Malm, K. Gebhart, D. Latimer, T. Cahill, R. Eldred, R. Pielke, R. Stocker, and J. Watson, "National Park Service Report on the Winter Haze Intensive Tracer Experiment," Final Report, National Park Service, Fort Collins, Colorado, December 4, 1989.
2. W. C. Malm, H. K. Iyer, J. Watson, and D. A. Latimer, "Survey of a Variety of Receptor Modeling Techniques," in this volume, 1990.
3. B. B. Hicks, "Dry Deposition Processes," in The Acidic Deposition Phenomenon and Its Effects. Critical Review Papers. Volume I. Atmospheric Sciences, EPA-600/8-83-016AF, U.S. Environmental Protection Agency, Washington D.C., 1984.

4. M. L. Wesely, "Parameterization of Surface Resistances to Gaseous Dry Deposition in Regional-scale Numerical Models. Atmos. Environ. 23, 1293-1304, 1989.
5. L. W. Richards, et al. "The Chemistry, Aerosol Physics, and Optical Properties of a Western Coal-fired Power Plant Plume," Atmos. Environ. 15, 2111, 1981.
6. J. H. Seinfeld, Atmospheric Chemistry and Physics of Air Pollution. John Wiley & Sons, New York, 1986.
7. B. J. Finlayson-Pitts and J. N. Pitts, Atmospheric Chemistry: Fundamentals and Experimental Techniques John Wiley & Sons, New York, 1986.
8. C. C. Van Valin, 1987. "Hydrogen Peroxide in Air During Winter Over the South-central United States," Geophysical Res. Letters. 14, 1146-1149, 1987.
9. S. V. Hering and S. K. Friedlander, "Origins of Aerosol Sulfur Size Distributions in the Los Angeles Basin. Atmos. Environ. 16, 2647, 1982.
10. P. H. McMurry and J. C. Wilson, "Growth Laws for the Formation of Secondary Ambient Aerosols: Implications for Chemical Conversion Mechanisms," Atmos. Environ. 19, 1445, 1982.

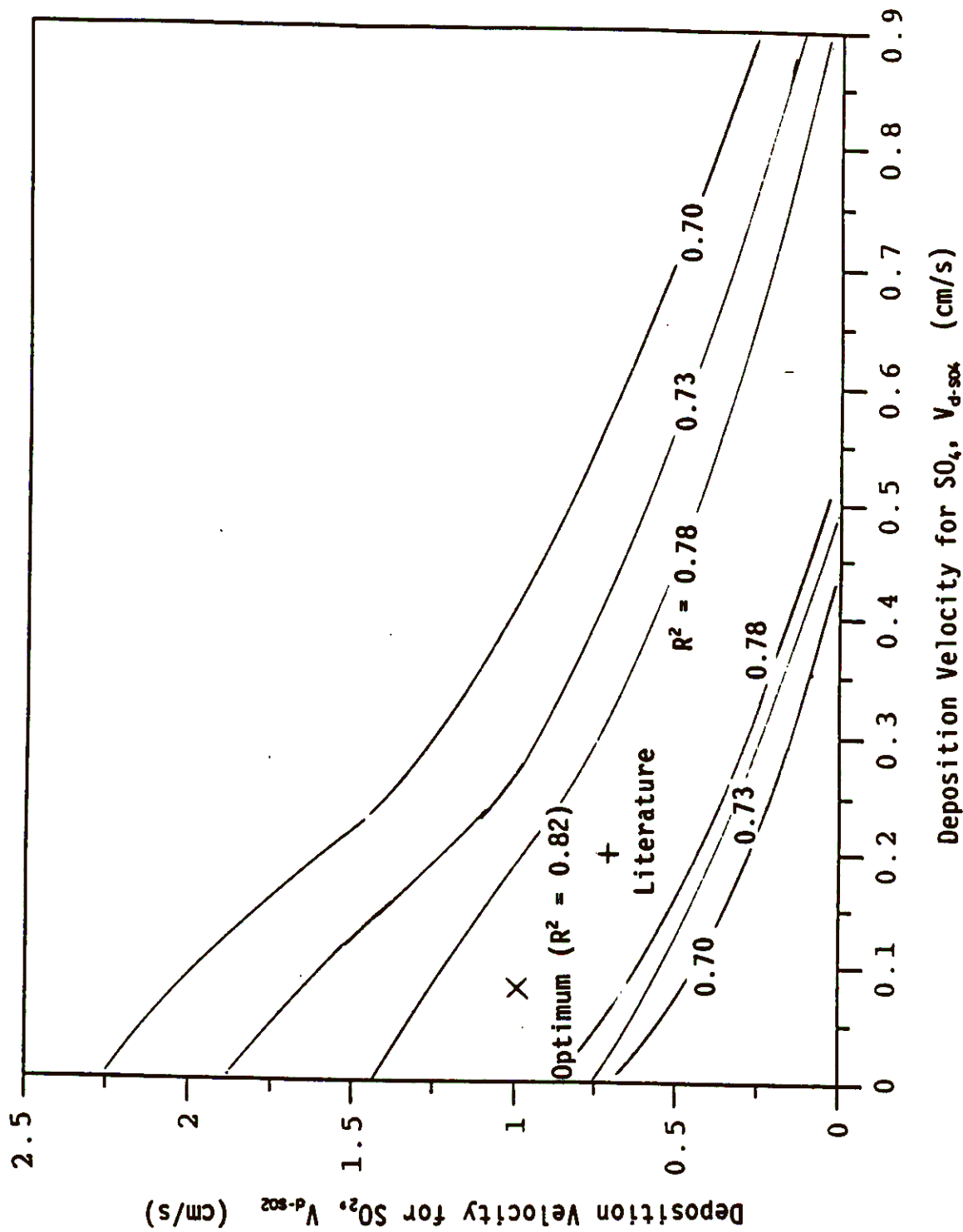


Figure 1. Combinations of deposition velocities for SO₂ and sulfate for an assumed SO₂ oxidation rate of 1.5%/h x RH/100, having $R^2 > 0.70$. (The optimized deposition rates are shown with an X, and the median of the literature values is shown with a +).

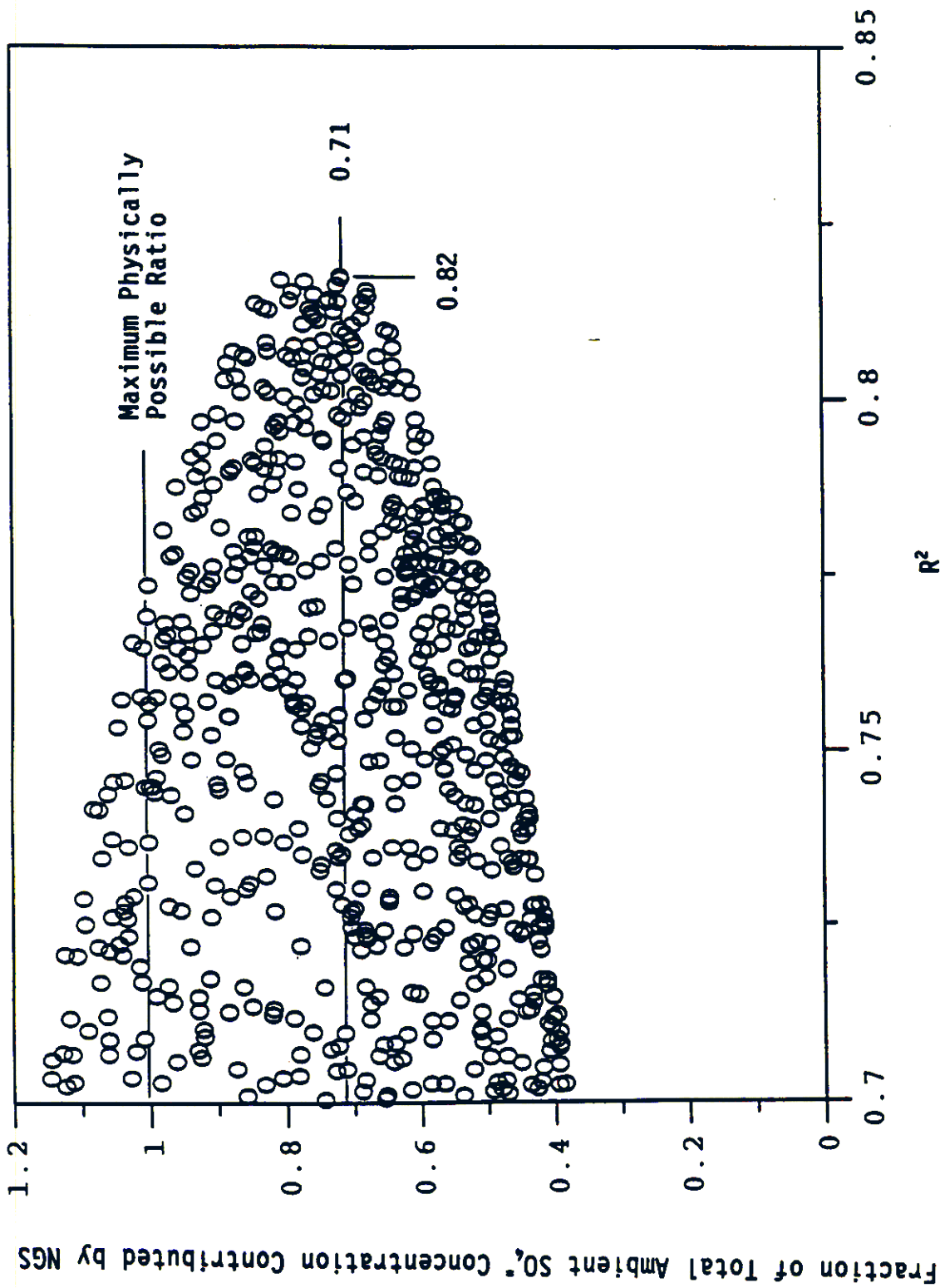
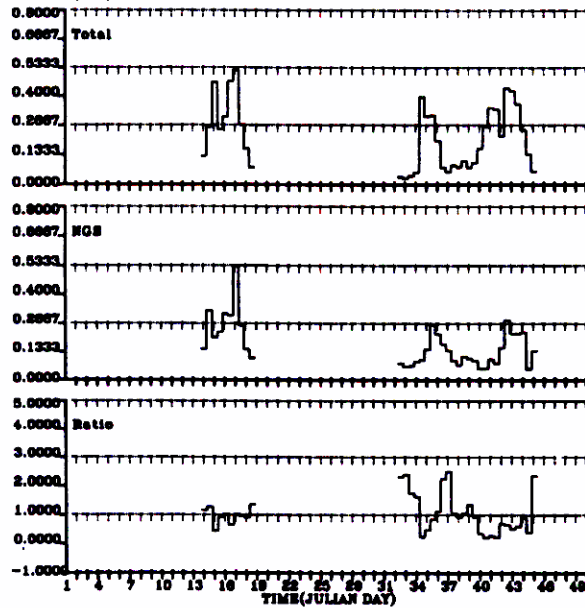


Figure 2. Calculated average NGS fraction of total ambient sulfate at Hopi Point in Grand Canyon National Park for all combinations of SO₂ and sulfate deposition velocities and SO₂ oxidation rates that yield R² > 0.70.

(a) Best estimates.



(b) Ranges of uncertainty.

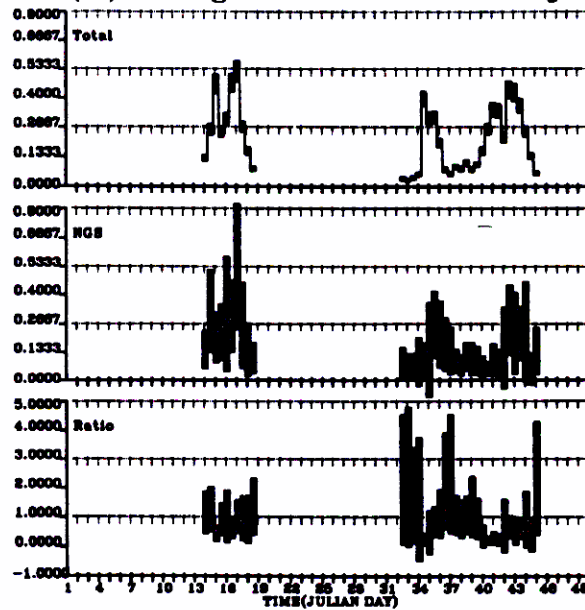


Figure 3. History of ambient sulfate sulfur ($\mu\text{g}/\text{m}^3$), sulfate sulfur due to NGS ($\mu\text{g}/\text{m}^3$), and the ratio of NGS to total ambient sulfate at Hopi Point.

Fraction of Emitted Sulfur

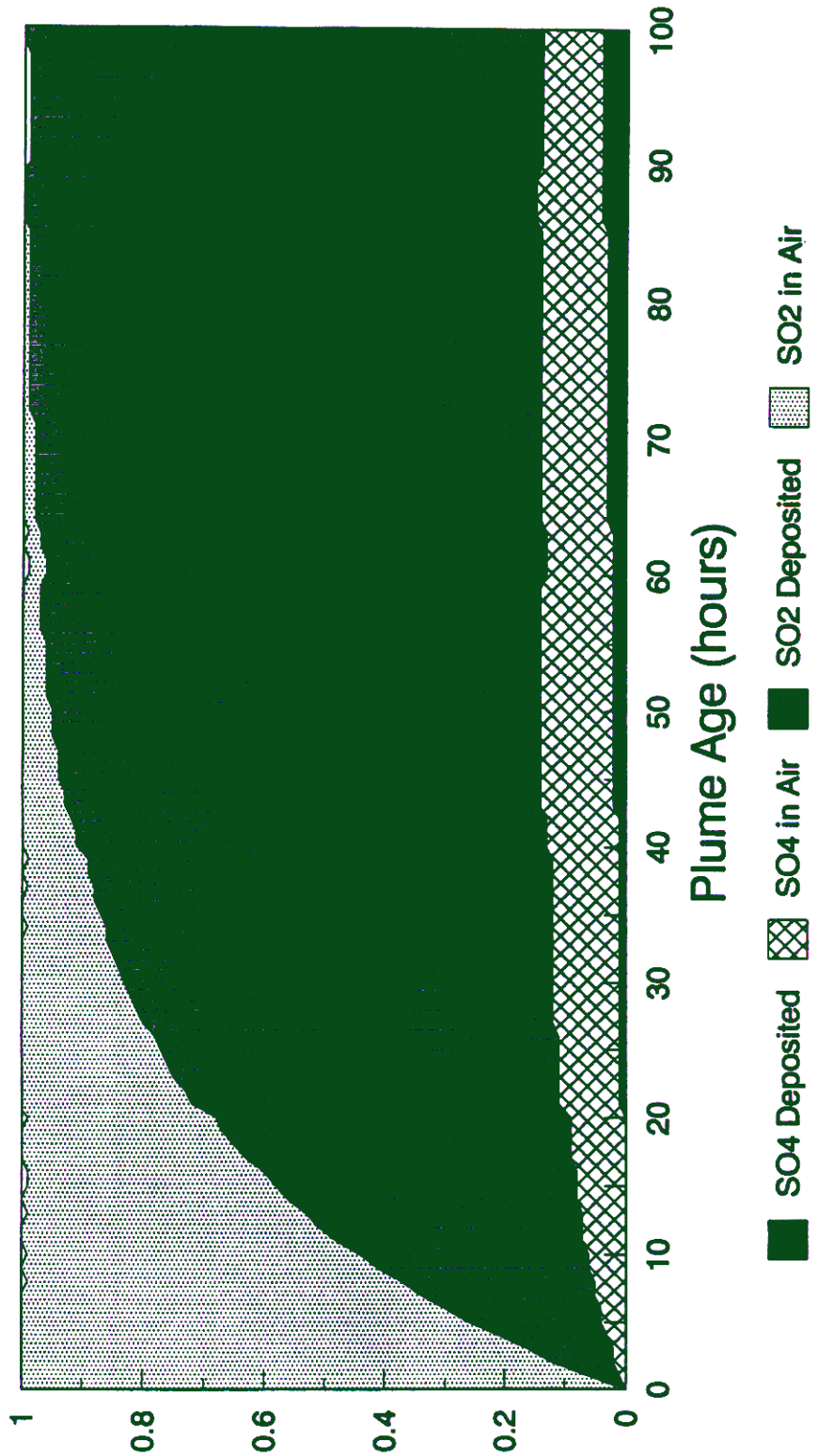


Figure 4. Oxidation and deposition of emitted sulfur as a function of plume age, based on the optimized DMB model.

Table I. History of measured total ambient and NGS SO_4^{2-} ($\mu g/m^3$), and the fraction of ambient sulfate due to NGS at Hopi Point, Grand Canyon National Park, based on the DMB model calculations.

Julian Day	Total Measured SO_4		NGS Contribution to SO_4			Fraction Due to NGS		
	Ambient SO_4 Concent	Uncertainty due to Measmt	NGS SO_4 Concent	Uncertainties due to K's	due to Measmt	Ratio	due to K's	due to Measmt
13.8	0.13	0.01	0.15	0.04	0.02	1.15	0.32	0.16
14.3	0.26	0.01	0.32	0.09	0.03	1.26	0.36	0.15
14.8	0.47	0.02	0.20	0.05	0.03	0.43	0.11	0.07
15.3	0.24	0.01	0.22	0.06	0.02	0.92	0.25	0.11
15.8	0.30	0.01	0.31	0.07	0.11	1.02	0.24	0.38
16.3	0.47	0.02	0.30	0.07	0.04	0.64	0.15	0.10
16.8	0.52	0.02	0.53	0.14	0.04	1.01	0.27	0.08
17.3	0.27	0.01	0.26	0.06	0.08	0.95	0.24	0.29
17.8	0.16	0.01	0.14	0.04	0.05	0.91	0.23	0.32
18.3	0.08	0.01	0.10	0.03	0.02	1.36	0.38	0.28
32.3	0.03	0.00	0.08	0.03	0.02	2.30	0.99	0.52
32.8	0.03	0.00	0.06	0.02	0.03	2.39	0.61	1.03
33.3	0.04	0.00	0.07	0.03	0.01	1.75	0.75	0.32
33.8	0.05	0.00	0.09	0.02	0.05	1.63	0.44	0.96
34.3	0.40	0.02	0.09	0.03	0.03	0.24	0.08	0.07
34.8	0.31	0.01	0.14	0.05	0.10	0.47	0.16	0.33
35.3	0.31	0.01	0.26	0.06	0.05	0.84	0.19	0.16
35.8	0.19	0.01	0.22	0.06	0.05	1.12	0.30	0.27
36.3	0.07	0.01	0.17	0.06	0.02	2.23	0.79	0.25
36.8	0.05	0.00	0.14	0.04	0.04	2.49	0.71	0.74
37.3	0.09	0.01	0.09	0.03	0.01	1.06	0.30	0.13
37.8	0.08	0.01	0.07	0.02	0.01	0.93	0.26	0.18
38.3	0.10	0.01	0.11	0.03	0.01	1.06	0.29	0.12
38.8	0.07	0.01	0.10	0.03	0.03	1.34	0.35	0.38
39.3	0.10	0.01	0.09	0.02	0.02	0.93	0.24	0.24
39.8	0.16	0.01	0.05	0.02	0.02	0.34	0.10	0.16
40.3	0.26	0.01	0.05	0.01	0.01	0.21	0.05	0.04
40.8	0.35	0.02	0.10	0.02	0.03	0.28	0.07	0.09
41.3	0.34	0.02	0.08	0.02	0.03	0.23	0.06	0.08
41.8	0.22	0.01	0.15	0.04	0.09	0.70	0.18	0.41
42.3	0.44	0.02	0.28	0.07	0.04	0.64	0.16	0.11
42.8	0.43	0.02	0.22	0.06	0.08	0.52	0.13	0.18
43.3	0.37	0.02	0.22	0.06	0.02	0.60	0.16	0.06
43.8	0.25	0.01	0.23	0.05	0.10	0.92	0.22	0.42
44.3	0.13	0.01	0.05	0.02	0.03	0.39	0.13	0.25
44.8	0.06	0.00	0.14	0.03	0.04	2.34	0.57	0.78